Energy 238 (2022) 121899

Contents lists available at ScienceDirect

Energy

journal homepage: www.elsevier.com/locate/energy

Thermal efficiency gains enabled by using CO_2 mixtures in supercritical power cycles

F. Crespi [a, *], P. Rodríguez de Arriba [a], D. Sánchez [a], A. Ayub [b], G. Di Marcoberardino [b], C.M. Invernizzi [b], G.S. Martínez [a], P. Iora [b], D. Di Bona [c], M. Binotti [d], G. Manzolini [d]

[a] Department of Energy Engineering, University of Seville, Seville, Spain
[b] Dipartimento di Ingegneria Meccanica e Industriale, Università Degli Studi di Brescia, Brescia, Italy
[c] LEAP S.c.a.r.l., Laboratorio Energia e Ambiente Piacenza, Piacenza, Italy
[d] Dipartimento di Energia, Poltiecnico di Milano, Milano, Italy

ARTICLE INFO

Article history:
Received 18 May 2021
Received in revised form
23 August 2021
Accepted 24 August 2021
Available online 28 August 2021

Keywords:
CO_2 Blends
CSP plant
SCARABEUS project
$_sCO_2$Power
Cycles supercritical CO_2

ABSTRACT

The present paper explores the utilisation of dopants to increase the critical temperature of Carbon Dioxide (sCO_2) as a solution towards maintaining the high thermal efficiencies of sCO_2 cycles even when ambient temperatures compromise their feasibility. To this end, the impact of adopting CO_2-based mixtures on the performance of power blocks representative of Concentrated Solar Power plants is explored, considering two possible dopants: hexafluorobenzene (C_6F_6) and titanium tetrachloride ($TiCl_4$). The analysis is applied to a well-known cycle -*Recuperated Rankine*- and a less common layout -*Precompression*-. The latter is found capable of fully exploiting the interesting features of these non-conventional working fluids, enabling thermal efficiencies up to 2.3% higher than the simple recuperative configuration. Different scenarios for maximum cycle pressure (250–300 bar), turbine inlet temperature (550–700 °C) and working fluid composition (10–25% molar fraction of dopant) are considered. The results in this work show that CO_2-blends with 15–25%(v) of the cited dopants enable efficiencies well in excess of 50% for minimum cycle temperatures as high as 50 °C. To verify this potential gain, the most representative pure sCO_2 cycles have been optimised at two minimum cycle temperatures (32 °C and 50°C), proving the superiority of the proposed blended technology in high ambient temperature applications.

1. Introduction

1.1. From the first steps to successful demonstration

The sCO_2 power cycle technology has triggered a growing interest in the scientific community in the last ten years. It currently stands out as the strongest alternative to steam turbines in the next generation of Concentrated Solar Power plants. Such interest is brought about by the higher thermal efficiency of the cycle and arguably smaller footprint of the equipment, features that were already recognised in the pioneering works by Angelino and Feher in the late sixties. The former author identified 650 °C as the break-even turbine inlet temperature (TIT) beyond which sCO_2 power cycles attain better thermodynamic performance than both air Brayton and water/steam Rankine cycles [1]. At the same time, Feher discussed the benefits of compressing sCO_2 in the vicinity of the critical point, taking advantage of the low compressibility factor in that region [2].

After a long period without interest in the technology, a large amount of research works have been published in the last fifteen years. In 2004, Vaclav Dostal's Ph. D thesis put sCO_2 in the spotlight again, identifying the *Recompression* and *Partial Cooling* sCO_2 cycles as the best candidates for IV Generation Nuclear reactors, capable of taking thermal efficiency close to 50% for a turbine inlet temperature of 650 °C [3]. A little later, the work carried out by the National Renewable Energy Laboratory explored advanced configurations of the same *Recompression* layout for CSP applications, adding intercooling and reheat and indeed confirming the potential of the cited cycle in this application [4,5]. This theoretical work received a crucial experimental support by SANDIA National Lab, whose first-of-a-kind experimental loop proved the benefits enabled by sCO_2 condensation in terms of turbomachinery design and operational

* Corresponding author.
E-mail address: crespi@us.es (F. Crespi).

https://doi.org/10.1016/j.energy.2021.121899

Nomenclature

ΔH_{is}	Turbine isentropic enthalpy variation [J/kg]
ΔP_{HX}	HX Pressure drop [%]
ΔT_{min}	Minimum temperature difference in HX [°C]
η_{is}	Isentropic Efficiency [%]
η_{th}	Cycle Thermal Efficiency [%]
CIT	Compressor Inlet Temperature [°C]
CSP	Concentrated Solar Power
h	Enthalpy [J/kg]
MW	Molar Weight [g/mol]
P_{cr}	Critical Pressure [bar]
P_{max}	Maximum Cycle Pressure [bar]
PIT	Pump Inlet Temperature [°C]
pp	Percentage point [%]
R_s	Specific Gas Constant [J/kgK]
s	Entropy [J/kgK]
SA	Simple Asphyxiant Gas [−]
SP	Turbine Size Parameter [m]
T_{cr}	Critical Temperature [°C]
TIP	Turbine Inlet Pressure [bar]
TIT	Turbine Inlet Temperature [°C]
V	Volumetric flow [m3/s]
v	Specific Volume [m3/kg]
VER	Volumetric Expansion Ratio [−]
W_c	Compression Work [J/kg]
WF	Working Fluid [−]
Z	Compressibility Factor [−]
~~W~~	React with water [−]

flexibility [6]. This has later been confirmed by experimental activities carried out by other institutions at the small scale [7,8].

From a commercial, larger-scale standpoint, the technology achieved a milestone when the Waste Heat Recovery Unit developed by Echogen was deployed to the market [9], becoming the first sCO_2 system to be ever commercialised. This was followed by the much larger system developed by NetPOWER and based on the Allam cycle. A 50 MWt oxy-combustion sCO_2 cycle running on natural gas started up in May 2019, demonstrating the unmatched capability of this technology to produce carbon-free electricity from fossil fuels [10].

1.2. First doubts and introduction to sCO_2 blends

Riding the wave of theoretical works developed in the first decade of the 21st century, the potential of the sCO_2 power cycle to enable thermal efficiencies higher than 50% in a variety of applications was widely acknowledged by the scientific community. Nevertheless, more detailed analyses published in recent years, and including not only thermal but also economic considerations, reveal that there are important challenges ahead of the technology.

For instance, as a common denominator, a large number of research works consider a fairly low temperature at compressor inlet, around 35 °C, in order to perform the compression process near the critical point. This is because the low compressibility factor of sCO_2 at such conditions enables a significant reduction of compression work, hence increasing thermal efficiency. Nevertheless, this assumption is utterly unrealistic for CSP applications, since sites with the very high solar resource needed (Direct Normal Irradiation) are usually located in desertic areas with ambient temperatures much higher than 35 °C. If higher minimum cycle temperatures (50 °C) are taken into account, thermal efficiency drops significantly and the potential gains with respect to conventional steam cycles become unclear. This is further discussed in a later section.

In the light of these considerations, the interest in the sCO_2 power cycle technology for CSP applications decreases largely as the performance gain with respect to state-of-the-art steam turbines and the technology readiness level (TRL) is reduced substantially.

Nevertheless, the addition of certain dopants to the raw carbon dioxide used in conventional sCO_2 cycles, yielding the so-called sCO_2 blends, has been identified by the SCARABEUS project as a groundbreaking route towards reverting this situation. Several authors have investigated this concept in the very last years: Invernizzi et al. studied the performance of Brayton cycles running on sCO_2 blended with various hydrocarbons [11], while Jeong et al. presented a similar study employing different gases (such as N_2, O_2 or He) as chemical dopants [12]. Bonalumi et al. claimed that employing a binary mixture of CO_2 and $TiCl_4$ in lieu of pure CO_2 could lead to efficiency gains as high as 5% and 3% in Brayton and *Recompression* cycle respectively [13]. Similarly, Baik et al. investigated the performance of Brayton cycles employing CO_2/R32 and CO_2/Toluene mixtures and confirmed that these working fluids enable better performance than pure sCO_2 at high heat sink temperatures [14]. Manzolini et al. investigated the use of N_2O_4 and $TiCl_4$ as chemical dopants in order to improve the efficiency of solar tower plants thereby reducing the cost of electricity associated to this technology [15]. Finally, as a further evidence of the increasing attention given by the scientific community to sCO_2 mixtures, it is worth noting that several works on this topic were recently presented at the 4th edition of the European sCO_2 Conference for Energy Systems [16].

It is in this context that the SCARABEUS project started in 2019, with the aim to demonstrate that the application of supercritical CO_2 blends to CSP plants has the potential to increase thermal efficiency above 50% when the minimum cycle temperature is as high as 50 °C. This enhancement of thermal performance comes along with a reduction of CAPEX by 30%, OPEX by 35% and LCOE to 96€/MWh, which is 30% below the current state-of-the-art steam-based CSP plants in a similar location [17].

Bearing all this in mind, the present paper aims to provide an assessment of the performance gain that could be expected from the utilisation of sCO_2 blends in CSP plants under realistic boundary conditions. To this end, the main concept of the SCARABEUS project is thermodynamically reviewed first. Then, the blends considered in this study are introduced, along with a brief description of the simulation tools used and of the two reference cycle layouts: *Recuperated Rankine* and *Precompression*. Finally, a comparison between the results obtained with the different mixtures is developed, with the aim to estimate the performance gains enabled by the adoption of the sCO_2-based blends as against a similar plant using steam turbines.

2. SCARABEUS project: concept

The enthalpy rise across a compression stage can be calculated through integration of Eq. (1). Assuming the process to be isentropic, Eq. (1) can be simplified and so compression work can be expressed as in Eq. (2), where the specific volume of the non-ideal working fluid depends on the compressibility factor Z. This relates the actual specific volume of the non-ideal gas to the specific volume of the gas at the same temperature and pressure, should it behave ideally.

$$dh = T\,ds + v\,dp \tag{1}$$

$$W_c = \int_1^2 v\,dp = \int_1^2 \frac{Z\,R\,T}{p}\,dp \tag{2}$$

Equation (2) suggests that compression work can be reduced if compressibility decreases, and this could potentially have a beneficial impact on cycle efficiency (all things being equal). This idea led Feher to propose a supercritical cycle [2] where compression takes place in the vicinity of the critical point with a liquid-like specific volume (i.e. a significantly lower specific volume and compressibility factor than in the gas phase). Unfortunately, a side-effect of working near this point is the large increase of the isobaric specific heat, which leads to a larger irreversibility in the recuperative heat exchanger. This was also identified by Angelino who, nevertheless, proposed different cycle layouts to overcome these problems related to heat transfer whilst still exploiting the compression work reduction [1].

Table 1 presents the impact of minimum temperature (bounded by ambient temperature) on cycle performance for a large number of sCO_2 cycle layouts. These layouts are taken from previous work by some of the authors, which provided a systematic approach to selecting pure sCO_2 cycles for CSP applications [18]. The cycles are modelled with Thermoflex software [19]. Two minimum temperatures are considered, 32 and 50 °C, whereas the maximum pressure and temperature of the cycle are set to 250 bar and 700 °C respectively. Isentropic efficiency is 93% and 89% for turbines and compressors respectively. All cycles have been optimised with the *SurrogateOpt* function in MatLab, recommended for time-consuming objective functions in order to reduce the computational time of the optimisation process [20]. The entire set of optimisation parameters is presented in Appendix A.

The trends observed in Table 1 come about because of the impact of compressor/pump inlet temperature on fluid compressibility, which rises rapidly when departing from the critical temperature, hence increasing compression work. For instance, for a compressor inlet pressure of 1.1 times the critical pressure, the compressibility factor increases from 0.28 to 0.65 when temperature changes from 34 to 61 °C [21]. Additionally, compressor outlet temperature increases more than proportionally due not only to the higher inlet temperature but, also, the higher compressibility. This means a lower potential for heat recovery in the cycle given that both turbine inlet temperature and pressure ratio remain the same for 32 and 50 °C. A significant efficiency drop is hence observed when raising this temperature from 32 °C (very close to the critical temperature) to 50 °C (more realistic value for usual CSP locations), regardless of cycle layout: between 2 and almost 5% points, depending on cycle configurations.

Two other observations can be made in addition to the evident detrimental effect of ambient temperature on cycle performance. On the one hand, most of the cycles in the comparison exhibit thermal efficiencies lower than 50%, the benchmark value considered in the SCARABEUS project. In particular, the *Simple Recuperated* and the *Modified Allam* layouts, the only sCO_2 cycles that have been tested extensively (even commercialised) to date, enable thermal efficiencies just slightly higher than steam Rankine cycles under similar boundary conditions (42%). On the other hand, those layouts achieving substantially higher efficiencies (in the order of 51%) imply very complex layouts which, in addition to compromising operability, also lead to significantly higher capital costs. This is the case of the *Recompression + IC + RH* and *Partial Cooling + RH* cycles which have been proved to be not cost effective in spite of their superior thermal performance [22].

In order to counteract the effects discussed in the previous section, the SCARABEUS project explores the opposite strategy. Rather than trying to reduce compressor inlet temperature to operate near the critical point, which is irremediably constrained by ambient conditions, the critical temperature of the working fluid is increased by adding dopants to the raw CO_2. This enables not only lower compressibility and compression work at high ambient temperatures, as in a standard sCO_2 cycle at low ambient temperature, but even condensation of the working fluid in the new boundary conditions. This has already been explored preliminarily by Di Marcoberardino et al. in the context of the SCARABEUS project [23]. These authors considered a mixture of CO_2 and C_6F_{14} in a cycle with condensation at 50 °C and a turbine inlet temperature of 400 °C, proving that thermal efficiency could be increased by 3–4% points with respect to pure sCO_2 if the appropriate dopant composition were used.

Table 1
Thermal efficiency of selected sCO_2 power cycles for two compressor inlet temperatures: 32 °C and 50 °C. Turbine inlet pressure and temperature are set to 250 bar and 700 °C. All cycles have been optimised for maximum thermal efficiency using MatLab's *SurrogateOpt* function.

Cycle layout	η_{th} [%] @ 32 °C	η_{th} [%] @ 50 °C	$\Delta\eta[pp]$
Simple Recuperated	46.7	44.7	2.0
Precompression	49.6	47.5	2.1
Recompression	53.7	49.3	4.4
Recompr.+IC + RH	54.9	51.9	3.0
Partial Cooling	52.8	49.1	3.7
Partial Cooling + RH	54.7	50.8	3.9
Modified Allam	47.5	45.9	1.6

3. Simulation tools

In order to study the impact of adopting sCO_2-based blends on the thermal performance of the power cycle, a series of simulations are run with the commercial software Thermoflex [19]. Two different cycles are considered, *Recuperated Rankine* and *Precompression*, whose layouts are provided in Fig. 1 along with their Temperature-entropy diagrams.

The former is a well-known configuration, adapted here to operate with sCO_2-blends whilst the *Precompression* layout originally proposed by Angelino [1] presents a somewhat unique and extremely interesting feature among the other sCO_2 power cycles. In contrast with other more popular configurations, such as *Recompression* or *Partial Cooling* (which present a flow-split before the low temperature recuperator in order to enhance thermal performance and avoid pinch-point problems), the potential of the *Precompression* layout lies on the addition of a compressor in the low-pressure side of the cycle, between the low and high-temperature recuperators. This particular feature overcomes the restriction imposed by the compression process on turbine exhaust pressure, thus enabling to control the compression and expansion ratios of the cycles separately. The additional degree of freedom can then be used to enhance thermal efficiency.

One of the critical tasks in SCARABEUS is to identify the optimal working fluid (dopant composition and molar fraction) that yields the largest thermal efficiency gain. To this aim, different dopants have already been studied by some of the authors [23] and some others are currently under investigation by the project partners. In this study, two of such dopants are considered: C_6F_6 (dopant D1) and $TiCl_4$ (dopant D2). The former is an organic, aromatic compound, characterised by low toxicity but high flammability and unconfirmed thermal stability at high temperatures. The latter is a

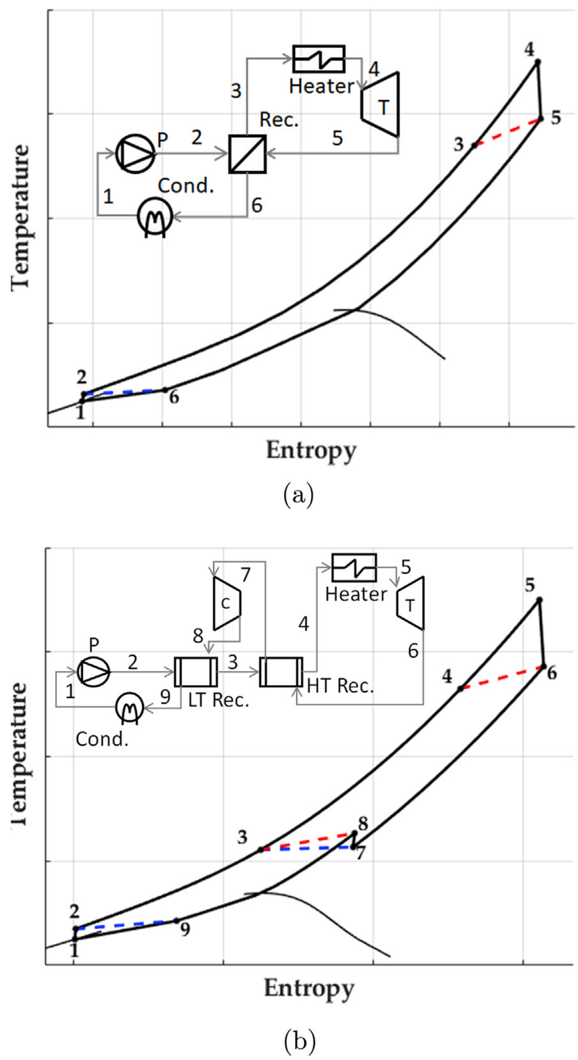

Fig. 1. *Recuperated Rankine* and *Precompression* cycles. Layouts and *T-s* diagrams. (a) Recuperated Rankine. (b) Precompression.

low cost fluid whose thermal stability has been proven at 550 °C, although it presents a very aggressive water reactivity, which may affect its actual feasibility at commercial scale. Further investigations regarding this particular aspect are currently undertaken by SCARABEUS consortium. A short evaluation of these two dopants in the context of NFPA 704 code is provided in Table 2.

With varying molar fractions of these two dopants, the blends in Table 3 are obtained, where X and YY in the blend code DXCYY stand for dopant D1/D2 and molar fraction (%) respectively. Table 3 also provides the saturation pressure of each blend corresponding to a bubble temperature of 50 °C; this latter temperature is set as the minimum cycle temperature of choice for cycle analysis. These two, 50 °C and Pcond are therefore the temperature and pressure at pump inlet (station 1 in both layouts in Fig. 1).

Table 2
Dopant hazard according to NFPA 704 [24].

	Health Hazard	Flammability	Chemical Reactivity	Special Hazard
sCO_2	2	0	0	SA
C_6F_6	1	3	0	–
$TiCl_4$	3	0	2	~~W~~

For each blend, the thermophysical properties of the mixture have been obtained with Aspen [25], employing the Peng-Robinson equation of state calibrated on experimental data of the corresponding Vapour-Liquid-Equilibrium (VLE) conditions [26,27]. Then, in order to integrate the properties of these non-conventional fluids into the Thermoflow library, look-up tables are produced with Aspen and used as input for the *User Defined Fluid* Tool of Thermoflex. This methodology provides a flexible and robust simulation environment for power cycles using sCO_2 blends.

It is worth noting that the critical conditions reported in Table 3 change significantly with blend composition, what gives room to tailoring the optimum working fluid to a given minimum cycle temperature (i.e., ambient temperature). The criterion to determine the feasible range of compositions that can be used in the cycles considered is thus based on the margin between critical temperature (Tcr) and temperature at pump inlet (T1), which is set to 30 °C in this work. Accordingly, for the T1 of choice, 50 °C, only those blends whose compositions yield critical temperatures higher than 80 °C are eligible; for instance, according to the information in Table 3, blends based on dopant D1 with a molar fraction lower than 10% do not meet this criterion and are, therefore, discarded. The same can be said for the dopant D2 with molar fraction lower than 15%. This possibility to adapt the composition of the blend to the desired pump inlet temperature turns out to be a very powerful feature of SCARABEUS, since different mixtures can be tailored to specific CSP locations (ambient conditions). This is highlighted in the concluding section.

The *Recuperated Rankine* and *Precompression* cycles have been modelled for all the sCO_2 blends in Table 3, for a Turbine Inlet Temperature of 550/700 °C and a maximum cycle pressure of 250/300 bar. For the resulting twenty-eight cases, the gross output of the cycle is 100 MW and the specifications of turbomachinery (isentropic efficiency) and heat exchangers (minimum pinch-point, pressure drops) are those summarised in Table 4.

4. Analysis of results

A thorough discussion on the actual potential of CO_2-blends to improve the thermal performance of sCO_2 power cycles is presented in this section. First of all, the combinations of blend and cycle layout enabling thermal efficiencies higher than 50% are identified. Then, the performance of cycles using these selected blends is analysed in detail in order to identify the root causes of the superior thermodynamic performance; this second step of the analysis is done for the case at 700 °C and 250 bar, herein considered as the most representative of SCARABEUS. Later, the dependence of the best combination of layout and blend on the operating and boundary conditions of the cycles is discussed. Finally, the influence of working fluid composition on the characteristics of certain equipment is investigated, with a particular focus on turbine and cooler/condenser.

4.1. Best combination of working fluid composition and cycle layout

The thermal efficiencies of the *Recuperated Rankine* and *Precompression* cycles for the entire set of boundary conditions presented in Table 4 are reported in Figs. 2 and 3 respectively. These are compared with the thermal efficiency of a state-of-the-art steam-based CSP plant (live steam temperature is set to 550 °C) and, for the sake of completeness, with an ultra-supercritical Rankine cycle (live steam pressure and temperature set to 300 bar and 625 °C/650 °C). These two reference values are reported in Figs. 2 and 3 with solid (labelled St.R) and dashed (labelled Usc. R) lines respectively.

The thermal efficiency of the *Recompression* cycle running on

Table 3
Specifications of CO_2 blends. Pcond is the condensation pressure corresponding to a bubble temperature of 50 °C.

Blend	Composition [% molar]	MW [g/mol]	Tcr [°C]	Pcr [bar]	Pcond [bar]
D1C10	CO_2–C_6F_6 [90–10]	58.21	80.28	112.4	83.50
D1C15	CO_2–C_6F_6 [85–15]	65.32	102.1	121.3	77.75
D1C20	CO_2–C_6F_6 [80–20]	72.42	121.9	123.6	71.83
D1C25	CO_2–C_6F_6 [75–25]	79.52	139.8	121.1	66.36
D2C15	CO_2–$TiCl_4$ [85–15]	65.86	93.76	190.9	96.88
D2C20	CO_2–$TiCl_4$ [80–20]	73.15	149.6	243.7	94.73
D2C25	CO_2–$TiCl_4$ [75–25]	80.43	192.0	247.1	91.39

Table 4
Boundary conditions and specifications of turbomachinery and heat exchangers.

PIT [°C]	TIT [°C]	Pmax [bar]	η_{is} [%] Pump/Turb/Compr
50	550/700	250/300	88/93/89
ΔT_{min} [°C]	ΔP_{heater} [%]	ΔP_{cond} [%]	ΔP_{rec} [%] Low P/High P
5	1.5	0	1/1.5

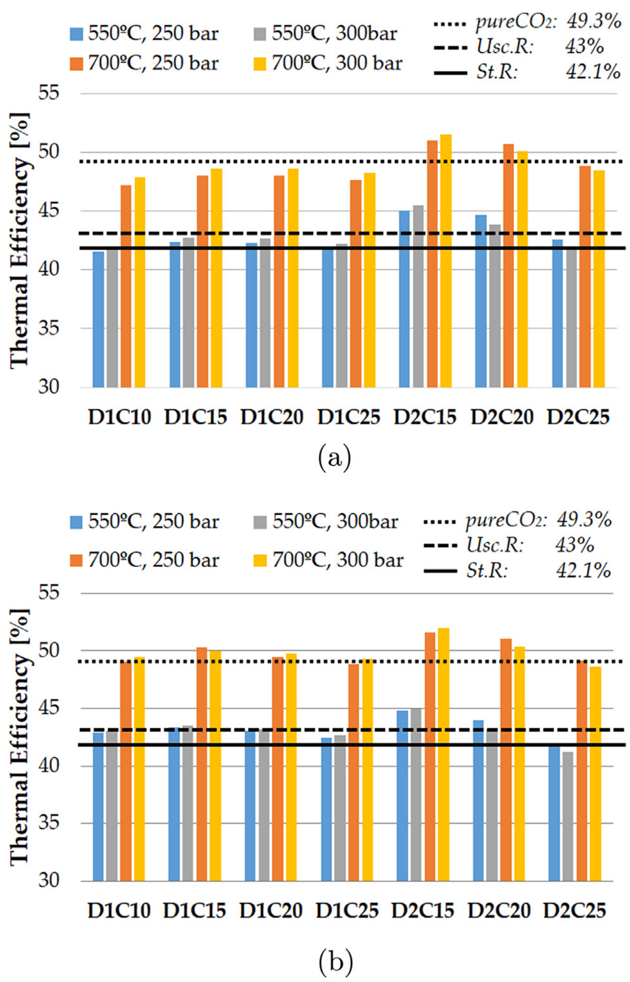

Fig. 2. Thermal efficiency of the *Recuperated Rankine* and *Precompression* cycles for different operating conditions and blends. (a) Recuperated Rankine. (b) Precompression.

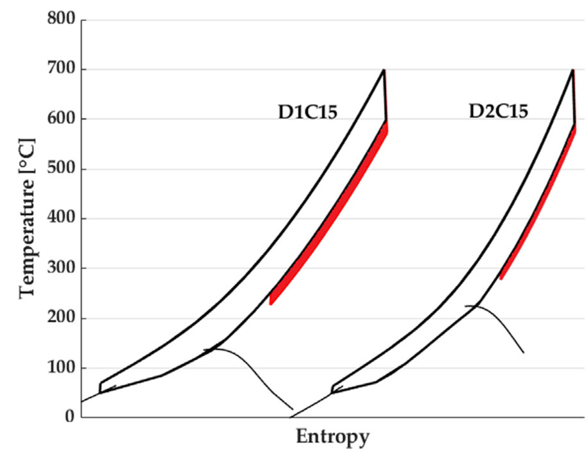

Fig. 3. *T-s* diagrams of the *Recuperated Rankine* (black) and *Precompression* (black + red) cycles considering D1C15 and D2C15. (For interpretation of the references to colour in this figure legend, the reader is referred to the Web version of this article.)

pure sCO_2 and a minimum cycle temperature of 50 °C is also reported in Figs. 2 and 3 with a dotted line (labelled pureCO_2). The value is taken from Table 1 and it is considered representative of the pure-sCO_2 power cycle technology at high ambient temperatures, capable of providing a good compromise between high thermal performance and overnight capital cost [22].

The information in Figs. 2 and 3 confirms that using sCO_2-blends enables better thermal efficiency than when pure sCO_2 or steam Rankine cycles are used. This becomes even more important in the light of the more complex (thus expensive) layout of conventional CSP plants with respect to the proposed solutions. As expected, it is also confirmed that the impact of increasing turbine inlet temperature on thermal efficiency is stronger than that of increasing maximum cycle pressure.

For the *Recuperated Rankine* cycle operating with CO_2–C_6F_6 mixtures (D1), the corresponding efficiency when TIT = 550 °C is comparable or even higher than for the standard steam Rankine cycle, and the difference increases dramatically when this temperature increases to 700 °C, even if compared against an ultra-supercritical steam cycle working at 625 °C/650 °C. For the best case in Fig. 2(a), given by D1C15 at 300 bar & 700 °C, the thermal performance of the *Recuperated Rankine* cycle is comparable to that of the *Recompression* layout working with pure sCO_2, even though the latter has a significantly more complex layout.

It is also interesting that CO_2–$TiCl_4$ mixtures (D2) present, for the most part, thermal efficiency higher than CO_2–C_6F_6 and, depending on operating conditions, the other technologies in Fig. 2(a) (sCO_2 and steam). Furthermore, amongst the D2CYY cases, the D2C15 blend yields the best performance, attaining a thermal efficiency well above 50% at 700 °C, thus outperforming all the other candidates by a large margin. This result is extremely interesting, bearing in mind that even if the complexity of the *Recuperated Rankine* cycle is similar to that of a Simple Recuperated (recuperated Brayton) cycle working on sCO_2, the former achieves much better performance; in particular, the efficiency of a

Recuperated Rankine cycle working on D2C15 at 700 °C (51%) is 6+ percentages higher than that of a *Simple Recuperated* (Brayton) cycle running on sCO_2 at the same turbine inlet temperature (44.7%).

Some comments about the better performance enabled by the specific features of the *Precompression* cycle, as reported in Fig. 2(b), are worth noting. As already highlighted for this cycle, turbine exhaust pressure is not constrained by condenser pressure, thanks to the incorporation of a compressor between the two recuperators (see Fig. 1). This increases the complexity but enables a much more flexible optimisation of compressor pressure ratio, regardless of turbine expansion ratio, after which thermal efficiency can be increased substantially. Indeed, utilising D1 blends in this cycle enables a thermal efficiency gain in the order of 2% points with respect to the base sCO_2 case, depending on the molar fraction of dopant and on the operating conditions. D1C10 and D1C15 yield the largest gains, 1.9pp and 2.3pp (at 250 bar & 700 °C), with the latter achieving 50.3% thermal efficiency and being the optimum mixture overall amongst the CO_2–C_6F_6 cases. It is worth noting that, for this combination of layout and blend, increasing the maximum pressure of the cycle hardly has any effect on η_{th} in spite of the significantly higher specific work (see Fig. 4(a)).

Using blends based on D2 in the *Precompression* cycle enables higher thermal efficiencies than the same fluid in the *Recuperated Rankine* but, in this case, the thermal efficiency rise is in the order of 0.5% point only. This happens when a D2C15 blend is used in cycles working at 250 bar and 700 °C, for which thermal efficiency increases from 51 to 51.6%. This is due to the different thermodynamic behaviour of this cycle when operated with different blends. The optimum pressure ratio of the precompressor (P_8/P_7 in Fig. 1(b)), in fact, happens to be greatly affected by the nature of the dopant employed, changing from 1.42 to 1.2 between D1C15 and D2C15. This pattern results in a larger relative improvement than for the *Recuperated Rankine* when sCO_2-C_6F_6 blends are considered, and it can be better observed by looking closer at the *T-s* diagrams in Fig. 3, for both D1C15 and D2C15 blends. The area depicted in black lines corresponds to the *Recuperated Rankine* cycle, while the *Precompression* layout is obtained when adding the area in red. This latter cycle has a larger area which stands for a higher specific work for the same heat addition, what also means higher efficiency of the *Precompression* layout; this is more visible for the D1C15 case. From these differences, the scenario described depicts a situation where the *Precompression* cycle steps forward as a better performing option overall, for which all the candidate mixtures achieve thermal efficiencies in the 50–52% range when running the cycle at 700 °C. For this cycle, adding a 15–20% molar fraction of C_6F_6 yields the best performance whereas 15% is best for mixtures based on $TiCl_4$.

The heat and mass balance sheets of a *Precompression* cycle operating with pure CO_2, D1C15 and D2C15 are reported in Tables 5–7, showing also the compressibility factors at each cycle station.

The beneficial influence of working fluid composition on thermal performance is now seen to be brought about by the effect of a lower compressibility across the compression stage (stations 1–2 in Fig. 1).

With regard to specific work (W_s), the *Precompression* cycle presents, as expected, a significantly higher W_s than the *Recuperated Rankine* cycle, owing to the higher expansion ratio enabled by the utilisation of a compressor between turbine outlet and pump inlet. This is shown in Fig. 4 where the impact of turbine inlet temperature and peak cycle pressure can also be assessed.

This figure also shows that both cycles and dopants exhibit similar W_s patterns for different blends: the blends with the smallest fraction of dopant (D1C10 and D2C15) always enable the highest specific work (for a given set of boundary conditions), and this decreases progressively as higher fractions are considered. For a given dopant, this is due to the increasing molar weight of the mixture, corresponding to an increasing circulating mass flow rate in the power cycle.

Generally speaking, $TiCl_4$-based (D2) blends present lower specific work than D1 mixtures, contrary to the pattern observed earlier for thermal efficiency. For this reason, a compromise between η_{th} and W_s is mandatory when selecting the best blend for a given cycle layout, even if the weight of thermal efficiency on this decision is expectedly much heavier than that of specific work.

4.2. Influence of operating conditions

Earlier sections of this work have revealed that D1C15 and D2C15 yield highest thermal efficiency for all the operating conditions taken into account and considering a minimum cycle temperature of 50 °C. This means that variations of either turbine inlet temperature or maximum cycle pressure do not have any influence

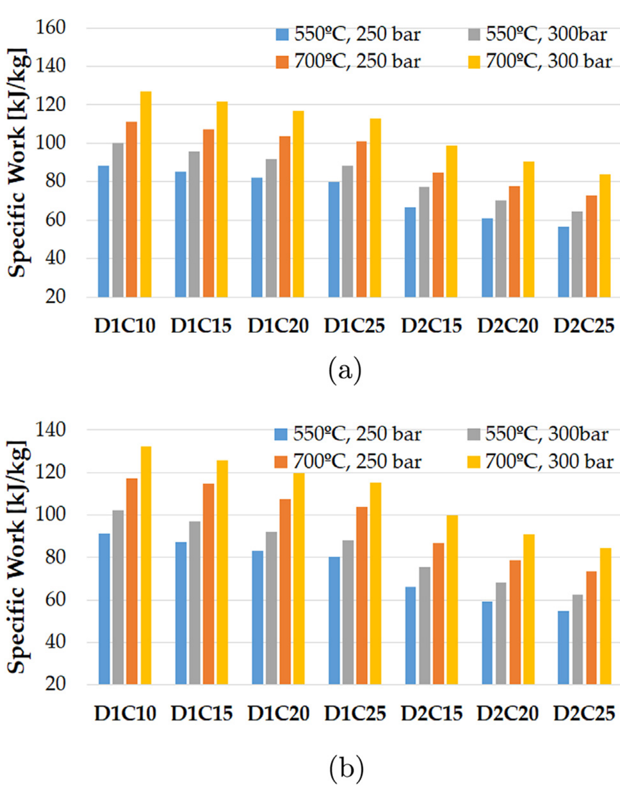

Fig. 4. Specific Work of the *Recuperated Rankine* and *Precompression* cycles for different operating conditions and blends. (a) Recuperated Rankine. (b) Precompression.

Table 5
Heat and mass balance of the *Precompression* cycle with pure CO_2. Compressor and turbine inlet temperatures are 50 °C and 700 °C. Maximum cycle pressure is 250 bar. Station numbers as per Fig. 1.

Cycle Station	T [°C]	P [bar]	h [kJ/kg]	s [kJ/kgK]	ρ [kg/m3]	Z [–]
1	50.0	135	−183	−1.37	655	0.337
2	71.8	250	−165	−1.36	728	0.527
3	193	246	67.6	−0.78	331	0.845
4	549	243	525	−0.04	150	1.044
5	700	239	716	0.18	123	1.054
6	586	105	580	0.19	63.4	1.017
7	198	104	123	−0.52	128	0.911
8	229	137	149	−0.51	157	0.921
9	78.0	136	−83.0	−1.07	377	0.544

Table 6
Heat and mass balance of the *Precompression* cycle with D1C15. Compressor and turbine inlet temperatures are 50 °C and 700 °C. Maximum cycle pressure is 250 bar. Station numbers as per Fig. 1.

Cycle Station	T [°C]	P [bar]	H [kJ/kg]	S [kJ/kgK]	ρ [kg/m3]	Z [−]
1	50.0	77.8	−7488	−1.476	893.9	0.211
2	71.1	250	−7468	−1.469	1004	0.568
3	234	246	−7203	−0.837	450.2	0.847
4	532	243	−6799	−0.206	225.8	1.049
5	700	239	−6570	0.055	180.3	1.069
6	571	56.9	−6729	0.069	51.64	1.007
7	239	55.3	−7134	−0.536	91.91	0.923
8	267	78.5	−7110	−0.531	124.0	0.921
9	87.6	77.8	−7374	−1.140	301.1	0.696

Table 7
Heat and mass balance of the *Precompression* cycle with D2C15. Compressor and turbine inlet temperatures are 50 °C and 700 °C. Maximum cycle pressure is 250 bar. Station numbers as per Fig. 1.

Cycle Station	T [°C]	P [bar]	h [kJ/kg]	s [kJ/kgK]	P [kg/m3]	Z [−]
1	50.0	96.9	−7020	−1.230	1079	0.220
2	64.9	250	−7004	−1.224	1143	0.513
3	277	246	−6698	−0.513	407.0	0.871
4	532	243	−6427	−0.105	230.7	1.034
5	700	239	−6259	0.087	183.7	1.058
6	570	82.3	−6374	0.097	76.86	1.007
7	282	81.5	−6645	−0.294	126.6	0.918
8	302	97.9	−6631	−0.292	146.1	0.922
9	71.9	96.9	−6938	−0.984	448.1	0.612

on this selection; i.e., the optimum blend remains the same regardless of further changes in these parameters. This conclusion is nevertheless not applicable to the minimum temperature of the cycle (pump inlet) whose variations impact which the optimum blend choice is. Given the dependence of this temperature on ambient temperature, this sets up a tight link between the location of the plant and the composition of the optimum blend.

In order to explore this further, a parametric analysis of the impact of ambient temperature on blend selection is performed for the *Recuperated Rankine* cycle. The results are provided in Table 8, where the performance of a *Simple Recuperated Brayton* working on pure sCO_2 at 250 bar and 700 °C is added for the sake of comparison.

There are several interesting aspects in Table 8. Remarkably, CO_2-blends prove to enable higher thermal efficiency than pure CO_2, employing a cycle with similar complexity. Nevertheless, an absolute best-performing blend regardless of minimum cycle temperature cannot be identified. Indeed, for the C_6F_6-based mixtures, D1C15 is found to yield the best performance for pump inlet temperatures equal or lower than 50 °C (best cases highlighted in bold). At higher temperatures, D1C20 becomes the best mixture of choice. On the other hand, considering mixtures based on $TiCl_4$, D2C15 yields the best performance for minimum cycle temperatures equal or higher than 40 °C whilst D2C20 becomes the best blend at lower temperature.

According to these results, the possibility to tailor the composition of the working fluid to the ambient conditions of the plant site in order to maximise performance becomes evident. This is an extremely powerful feature of this study, which goes beyond the application of the concept to Concentrated Solar Power plants and paves the way for the further optimisation of supercritical power cycles using CO_2 blends in other applications (for instance nuclear or waste heat recovery applications).

4.3. Impact on component performance and design

In this section, interesting aspects of component design and performance are discussed. For the turbine, two parameters are usually employed to preliminarily assess design and manufacturability: Volumetric Expansion Ratio (VER) and Size Parameter (SP) [28]. The former is defined as the ratio from specific volume at turbine outlet to specific volume at turbine inlet, assuming isentropic expansion, Eq. (3)a.

$$VER = \frac{v_{4s}}{v_3} \tag{3}$$

$$SP = \frac{\sqrt{\dot{V}_{4s}}}{\Delta h_{is}^{1/4}} \tag{4}$$

Large values of this parameter imply large area variations across the turbine which, inevitably, lead to larger aerodynamic losses and a larger number of stages to accommodate the large density variations. Therefore, the volumetric expansion ratio provides a qualitative indication of the expected isentropic efficiency and stage count of the turbine.

The size parameter is defined as the ratio from the square root of the volumetric flow at turbine outlet to the enthalpy change across the turbine (Δh_{is}) to the power of 0.25, in both cases assuming an isentropic expansion. This parameter is linked to turbine size, thus being a suitable indicator to compare size (and cost, for a given set of boundary conditions) of turbines operating with different blends and it is also linked to turbine efficiency. Turbines with smaller size parameters are more likely to suffer from tip leakage losses and low Reynolds number effects. Therefore, all things being equal, one would be interested in cycles and blends yielding low volumetric expansion ratios and high size parameters, in order to achieve the highest turbine efficiency.

These two parameters are reported in Table 9 for the reference *Recuperated Rankine* cycle working at 250 bar and 700 °C. The VER values reported are low regardless of the mixture, which confirms that the aerodynamic design of the turbine is not challenging in terms of a largely three-dimensional flow. Nevertheless, in spite of this favourable VER overall, it is interesting to verify that the

Table 8
Thermal efficiency ([%]) of the Recuperated Rankine for different blends and pump inlet temperatures.

PIT	30 °C	35 °C	40 °C	45 °C	50 °C	55 °C	60 °C
CO_2	–	46.6	45.0	45.3	44.7	44.2	43.7
D1C10	50.81	49.92	49.04	48.13	47.21	46.32	45.46
D1C15	**50.98**	**50.27**	**49.53**	**48.78**	**48.04**	47.30	46.62
D1C20	50.55	49.92	49.29	48.66	48.03	**47.43**	**46.83**
D1C25	49.84	49.29	48.74	48.20	47.67	47.16	46.66
D2C15	53.48	52.90	**52.31**	**51.67**	**50.98**	**49.97**	**48.95**
D2C20	**53.61**	**52.96**	52.28	51.53	50.65	49.73	48.73
D2C25	51.39	50.84	50.19	49.52	48.81	48.06	47.26

Table 9
Volumetric expansion ratio and size parameter for a Recuperated Rankine cycle operating at 250 bar and 700 °C with CO_2-TiCl_4 than for the $CO_2-C_6F_6$ blends.

Blend	VER [−]	SP [m]
D1C10	2.410	0.1876
D1C15	2.591	0.1893
D1C20	2.800	0.1920
D1C25	3.023	0.1948
D2C15	2.073	0.2001
D2C20	2.114	0.2041
D2C25	2.178	0.2123

addition of larger fractions of dopant has the effect of increasing the volumetric expansion ratio due to the higher molecular weight of the resulting mixture. The size parameter is higher values for CO_2-TiCl_4 than for the $CO_2-C_6F_6$ blends, contrary to VER, and it also exhibits a proportional increase with the molar fraction of dopant. In any case, the values of both VER and SP in Table 9 suggest that the aerodynamic design of turbines for the cases analysed does not pose large challenges (as far as the annulus is concerned). Similar results were obtained by City, University of London, in a recent publication linked to the SCARABEUS Project [29].

Cooler design and operation stems as one of the most critical tasks to undertake in CSP plants, usually located in desertic areas with extremely high ambient temperatures. This becomes even more challenging if condensing cycles are considered and if the use of air-cooled condensers turns out mandatory due to water scarcity.

In state-of-the-art CSP plants using steam turbines, the flow entering the condenser is partly in liquid state already: typically, 10%–15% of the turbine exhaust flow has already condensed inside the turbine. This is somewhat similar to what happens when CO_2-based blends are used: part of the fluid entering the condenser is already in liquid state. Nevertheless, in this case, this previous condensation does not take place inside the turbine but across the low-pressure side of the low-temperature recuperator. The beneficial aspect of this condensation upstream of the condenser, which can be observed in the heat and mass balance provided in Table 6, is a reduction of the duty of this component, what lowers not only its cost but also the auxiliary power needed to reject heat to the environment. It is also worth noting in this regard that the particular composition of the CO_2 blend used in the cycle has an impact on steam quality at condenser inlet and, accordingly, on condenser duty. This is shown in Fig. 5 where the blue and yellow bars stand for specific and overall duty of the condenser (left axis) whereas inlet quality is reported by the black markers (right axis). The values apply to a *Recuperated Rankine* cycle operating at 250 bar and 700 °C, with 50 °C pump inlet temperature and a power output of 100 MW.

In the chart, quality at condenser inlet and specific duty show a decreasing trend for increasing molar fraction. This pattern suggests that the use of mixtures of a higher dopant fraction could reduce the specific duty of the condenser, hence reducing the associated auxiliary power and cost. Nevertheless, a look at the absolute duty reveals that this metric is almost constant for all D1 blends whereas it increases slightly at higher molar fractions of dopant for D2 mixtures. This is, of course, due to the counteracting effect of a visibly higher mass flow rate for increasing dopant concentration, as shown in Fig. 6; this could have also been deduced from the specific work patterns in Fig. 4(a), in a context where cycle output (MW) remains constant. In summary, the reduction in condenser specific duty cannot counterbalance the effect of the increased circulating mass flow and, therefore, does not necessarily correspond to smaller equipment.

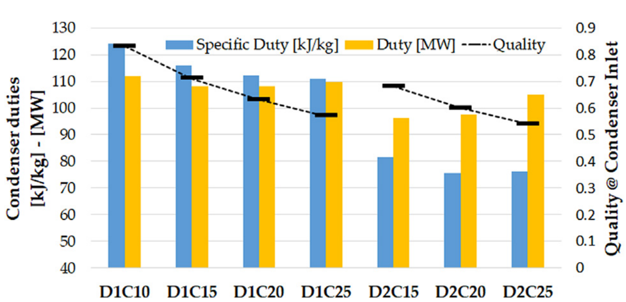

Fig. 5. Specific and absolute condenser duty (left axis) and fluid quality at condenser inlet (right axis) of a 100 MW *Recuperated Rankine* cycle operating at 250 bar and 700 °C.

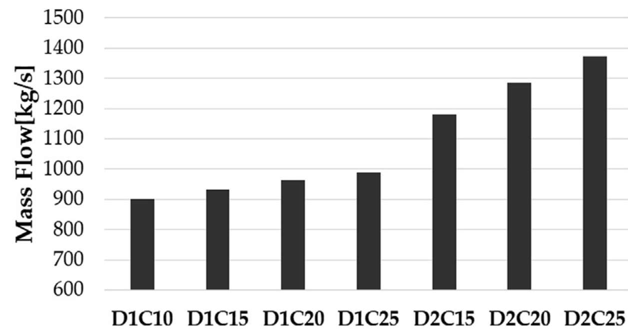

Fig. 6. Circulating mass flow of a 100 MW *Recuperated Rankine* cycle operating at 250 bar and 700 °C.

Overall, it is confirmed that peak thermal efficiency is provided by the blends for which the absolute duty of the condensers, for given gross cycle output, is minimum (as it was to be expected).

5. SCARABEUS: a paradigm shift

It has already been stated in earlier sections that thermal efficiency of the cycle is generally enhanced when shifting from a *Recuperated Rankine* cycle to a *Precompression* cycle. However, the thermal efficiency variation experienced in this move is not homogenous; rather, it happens to depend strongly on the working fluid considered. This is clearly observed in Table 10 which has a seemingly irregular pattern. The reason for this pattern is actually found in the fundamental thermodynamic behaviour of the cycles, which depends itself on the different thermophysical properties of the various candidate mixtures.

At a macro-scale, the thermal efficiency enabled by $TiCl_4$ mixtures in a *Recuperated Rankine* cycle, Table 8, proved to be higher than when using C_6F_6. Now, Table 10 reveals that the performance gain brought about by the adoption of the *Precompression* layout is larger for C_6F_6 blends than for cases based on $TiCl_4$. From a different angle, this indicates that, despite starting from a lower efficiency, $CO_2-C_6F_6$ mixtures seem to have a larger margin for performance improvement out of modifications of cycle layout than CO_2-TiCl_4. In some cases, correspondent to TIT of 550 °C, the thermal efficiency gains observed by $TiCl_4$-based mixtures result to be even negative, meaning that the *Recuperated Rankine* cycle seems to be able to better exploit the potential of these blends at such boundary conditions.

As a consequence of this, the more relevant conclusion of this work, second to the very high efficiencies enabled by CO_2 blends, is the new approach to the design of supercritical cycles using these mixtures. Indeed, the optimisation of working fluid composition for a given dopant and set of boundary and operating conditions does

Table 10
Thermal efficiency gains (additional percentage points) when shifting from a *Recuperated Rankine* cycle to a *Precompression* cycle for the given operating conditions.

Blend	550 °C 250 bar	550 °C 300 bar	700 °C 250 bar	700 °C 300 bar
D1C10	+1.35	+1.03	+1.90	+1.56
D1C15	+1.03	+0.79	+2.27	+1.35
D1C20	+0.77	+0.59	+1.38	+1.18
D1C25	+0.61	+0.45	+1.20	+1.05
D2C15	**−0.23**	**−0.47**	+0.62	+0.40
D2C20	**−0.66**	**−0.65**	+0.39	+0.27
D2C25	**−0.73**	**−0.75**	+0.33	+0.19

not make sense anymore or, to say it better, is incomplete. In order to really accomplish full optimisation for a given dopant and boundary conditions, leading to the attainment of the highest efficiency possible, it is mandatory to perform a simultaneous optimisation of cycle layout and fluid composition. This approach to cycle optimisation is currently under development at University of Seville for the SCARABEUS project although, at this stage, more research is still needed to fully understand the behaviour of CO_2-based blends in different cycle configurations. If confirmed, this paradigm shift would certainly pave the way for a more flexible and comprehensive understanding of sCO_2 power cycles technology development.

6. Conclusions

This work has investigated the actual potential of CO_2-based blends to enhance the performance of sCO_2 power cycles when applied to boundary and operating conditions characteristic of Concentrating Solar Power applications. The objective of the assessment, set forth at the beginning of the paper, was to verify the performance gains that could be attained thanks to the utilisation of working fluids incorporating carbon dioxide and different dopants with the overall effect to shift the pseudocritical temperature of the resulting mixture to a value higher than the critical temperature of CO_2.

With this in mind, two different dopants have been studied, C_6F_6 and $TiCl_4$, with molar fractions ranging from 10 to 25%, and their performances have been assessed in two cycle layouts, *Recuperated Rankine* and *Precompression*. In both cases, minimum cycle temperature (temperature at pump inlet) has been set to 50 °C, corresponding to an intermediate-high ambient temperature representative of typical CSP locations. For the sake of completeness, the maximum pressure and temperature of the working fluid have been changed in a range of interest as well.

The assessment described in the afore-described framework yields the following conclusions:

- For a given minimum cycle temperature, there is a minimum molar fraction of dopant below which condensation is not feasible. This sets a lower limit of dopant concentration which is specific to each dopant composition. For the dopants considered in this analysis and a PIT of 50 °C, this lower limit is found between 10 and 15%.
- Using CO_2-based mixtures in supercritical cycle layouts proves to enable η_{th} well in excess of 50%, even for ambient temperatures as high as 50 °C. This is well above what state-of-the-art Rankine cycles running on steam are currently achieving in CSP plants, thus meaning an unprecedented upsurge in performance for this type of application.
- This performance of supercritical cycle layouts using CO_2-based mixtures is also much better than what conventional supercritical CO_2 can attain for the same boundary conditions. This is due to the deleterious effect of high ambient temperatures on the compression process in the latter cycles. The gain enabled CO_2-based mixtures is in the order of 4–5% points with respect to an equivalent embodiment with pure CO_2 (more than 10% relative performance improvement).
- The performance of supercritical cycle layouts using CO_2-based mixtures shows a weak dependence on turbine inlet pressure whereas the influence of minimum and maximum cycle temperatures is very strong. Nevertheless, regarding temperature, whilst both temperatures determine thermal efficiency, turbine inlet temperature does not have any influence on the composition of the blend yielding the best performance. This seems to be dependent on minimum cycle temperature only.
- Component design, in particular turbine design, seems to be not compromised by the utilisation of the new WFs.
- When CO_2-based mixtures are used, cycle optimisation must include WF composition and cycle layout as independent variables. This is because the layout yielding the best η_{th} changes as mixture composition changes.

In addition to the specific conclusions listed above, there are two main, general conclusions drawn from this work. First and foremost, the discussion in this work confirms that achieving thermal efficiencies well in excess of 50% at attainable turbine inlet temperatures is now possible. This is because the CO_2-blend concept overcomes the main Achilles' heel of conventional supercritical CO_2 power cycles. Second, CO_2 mixtures pave the way for new CSP plants which can actually be tailored to the boundary conditions that are specific to each CSP plant. In other words, fluid composition and cycle layout could be tuned specifically to these boundary conditions in order to squeeze the thermodynamic potential of the concept as much as possible.

Further research by the authors will search new dopants and cycle layouts that could bring even larger gains whilst also developing new optimisation strategies that can automate this decision making process.

Declaration of competing interest

The authors declare that they have no known competing financial interests or personal relationships that could have appeared to influence the work reported in this paper.

Acknowledgements

The SCARABEUS project has received funding from the European Union's Horizon 2020 research and innovation programme under grant agreement N 814985. The University of Seville is also gratefully acknowledged for supporting this research through its Internal Research Programme (Plan Propio de Investigación), under contract No 2019/00000359.

Credit author statement

Francesco Crespi: Conceptualization, Methodology, Software, Formal Analysis, Data curation, Writing – Original Draft, Writing – Review and Editing, Visualization. **Pablo Rodríguez de Arriba**: Methodology, Software, Data curation, Writing – Original Draft. **David Sánchez**: Conceptualization, Writing – Review and Editing, Visualization, Supervision, Project Administration. **Abubakr Ayub**: Methodology, Formal Analysis. **Gioele di Marcoberardino**: Methodology, Investigation. **Costante Invernizzi**: Methodology, Formal Analysis, Resources, Supervision. **Gonzalo Sánchez Martínez**: Methodology, Software. **Paolo Iora**: Methodology, Investigation. Daniele Di Bona: Resources, Investigation. **Marco Binotti**: Supervision, Funding acquisition. **Giampaolo Manzolini**: Supervision, Funding acquisition.

Appendix A. Pure sCO_2 cycles optimised parameters

The supercritical Carbon Dioxide cycles in Table 1 are modelled with the boundary conditions of Table A.11. These are identical to those in Table 4, with the only exception of the pressure drops across the Heat Rejection Unit, neglected for condensing cycles using sCO_2-blends.

Table A.11
Boundary conditions and specifications of turbomachinery and heat exchangers of sCO_2 cycles.

Tmin [°C]	TIT [°C]	Pmax [bar]	η_{is} [%] Turb/Compr
32/50	700	250	93/89
ΔT_{min} [°C]	ΔP_{heater} [%]	ΔP_{cond} [%]	ΔP_{rec} [%] Low P/High P
5	1.5	1	1/1.5

Once these boundary conditions are set, the remaining parameters of the cycle are optimised in order to attain highest (cycle) thermal efficiencies: minimum and intermediate pressures (all configurations) and split-flow factor α (part-flow configurations: *Recompression*, *Partial Cooling* and derived layouts). For the sake of simplicity, the foregoing parameters are provided here for given pressure ratios of the different compressors and for the expansion ratio of the reheat turbine. The actual pressures can be calculated easily by considering that maximum pressure is set to 250 bar.

The entire set of optimised parameters is reported in Table A.12 whilst cycle layouts are presented in Figure A.7 in order to enhance readability of the paper.

Table A.12
Optimum operating parameters of different sCO_2 cycles considering two minimum cycle temperatures.

		α [−]	C1 PR [−]	C2 PR [−]	C3 PR [−]	T2 ER [−]
1) Simple Recuperated	**32°C**	–	3.333	–	–	–
	50°C	–	3.072	–	–	–
2) Precompression	**32°C**	–	2.313	1.450	–	–
	50°C	–	1.849	1.326	–	–
3) Recompression	**32°C**	0.373	3.255	–	–	–
	50°C	0.292	2.451	–	–	–
4) Partial Cooling	**32°C**	0.442	1.508	3.222	–	–
	50°C	0.406	1.761	2.270	–	–
5) Recompression + IC + RH	**32°C**	0.383	1.200	2.779	–	1.810
	50°C	0.335	1.753	2.366	–	1.904
6) Partial Cooling + RH	**32°C**	0.437	1.931	3.228	–	2.622
	50°C	0.401	1.999	2.323	–	2.150
7) Modified Allam	**32°C**	–	1.246	1.236	3.148	–
	50°C	–	1.220	1.285	2.940	–

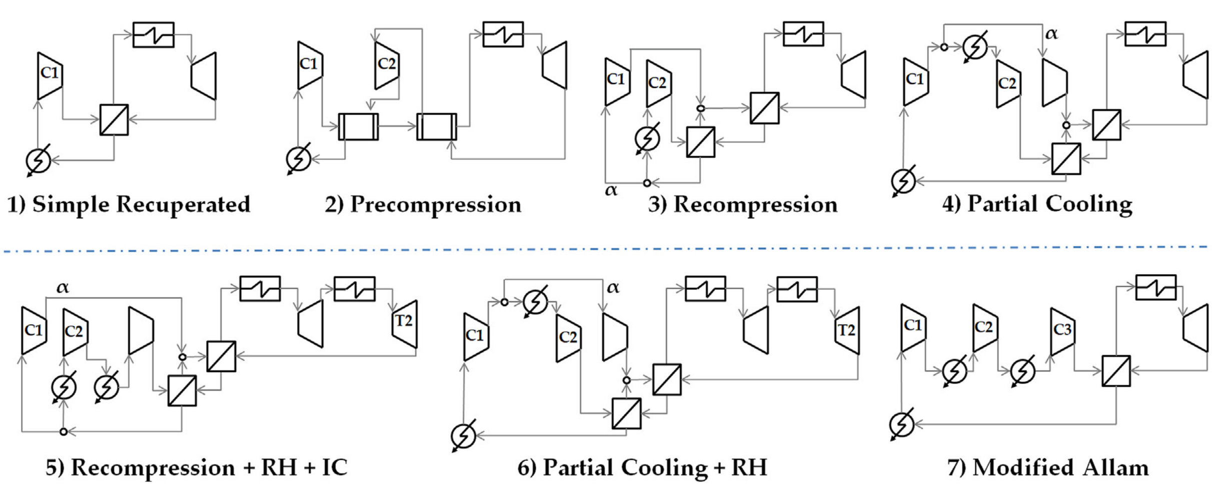

Fig. A.7. Layouts of different pure-sCO_2 cycles.

References

[1] Angelino G. Real gas effects in carbon dioxide cycles 79832. 1969.
[2] Feher EG. The supercritical thermodynamic power cycle. Energy Convers 1968;8:85–90.
[3] Dostal V, Driscoll MJ, Hejzlar P. A supercritical carbon dioxide cycle for next generation nuclear reactors. 2004.
[4] C. S. Turchi, Z. Ma, J. Dyreby, Supercritical carbon dioxide power cycle configurations for use in concentrating solar power systems, in: Turbo Expo: Power for Land, Sea, and Air, volume 44,717, American Society of Mechanical Engineers, pp. 967–973.
[5] T. Neises, C. S. Turchi, Supercritical co2 power cycles: design considerations for concentrating solar power, in: 4th international symposium—supercritical CO2 power cycles, Pittsburgh, PA, Sept, Citeseer, pp. 9–10.
[6] Wright SA, Radel R, Conboy T, Rochau GE. Modeling and experimental results for condensing supercritical co2 power cycles. Jan: Sandia Report; 2011.
[7] K. J. Kimball, E. M. Clementoni, Supercritical carbon dioxide brayton power cycle development overview, in: Turbo Expo: power for Land, Sea, and air, volume vol. 44717, American Society of Mechanical Engineers, pp. 931–940.
[8] J. Cho, H. Shin, H.-S. Ra, G. Lee, C. Roh, B. Lee, Y.-J. Baik, Development of the supercritical carbon dioxide power cycle experimental loop in kier, in: ASME Turbo Expo 2016: turbomachinery technical conference and exposition, American Society of Mechanical Engineers Digital Collection.
[9] Persichilli M, Held T, Hostler S, Zdankiewicz E, Klapp D. Transforming waste heat to power through development of a co2-based-power cycle. Electric Power Expo 2011;10.
[10] NET Power's clean energy demonstration plant. Texas: La Porte; 2016. accessed May 12th 2021, https://www.power-technology.com/projects/net-powers-clean-energy-demonstration-plant-la-porte-texas/.
[11] Invernizzi CM, van der Stelt T. Supercritical and real gas brayton cycles operating with mixtures of carbon dioxide and hydrocarbons. Proc IME J Power Energy 2012;226:682–93.
[12] Jeong WS, Lee JI, Jeong YH. Potential improvements of supercritical recompression co2 brayton cycle by mixing other gases for power conversion system of a sfr. Nucl Eng Des 2011;241:2128–37.
[13] Bonalumi D, Lasala S, Macchi E. Co2-ticl4 working fluid for high-temperature heat source power cycles and solar application. Renew Energy 2020;147: 2842–54.
[14] S. Baik, J. I. Lee, Preliminary study of supercritical co2 mixed with gases for power cycle in warm environments, in: Turbo Expo: power for Land, Sea, and air, volume vol. 51180, American Society of Mechanical Engineers, p. V009T38A017.
[15] Manzolini G, Binotti M, Bonalumi D, Invernizzi C, Iora P. Co2 mixtures as innovative working fluid in power cycles applied to solar plants. techno-economic assessment. Sol Energy 2019;181:530–44.
[16] prague Carbon dioxide mixtures at the 4th european sco2 conference for energy systems. 2021. July 7th 2021, https://www.scarabeusproject.eu/2021/05/04/the-4th-european-s-co2-conference-for-energy-systems/.
[17] Supercritical CARbon dioxide/alternative fluids blends for efficiency upgrade of solar power plants. 2019. May 12th 2021, https://cordis.europa.eu/project/rcn/221766/factsheet/en.
[18] Crespi F, Gavagnin G, Sánchez D, Martínez GS. Analysis of the thermodynamic potential of supercritical carbon dioxide cycles: a systematic approach. J Eng Gas Turbines Power 2018;140.
[19] Thermoflow inc, Thermoflow suite - Thermoflex software. accessed May 12th 2021, https://www.thermoflow.com/products_generalpurpose.html, 2021. Online.
[20] Surrogate optimization for global minimization of time-consuming objective functions, https://es.mathworks.com/help/gads/surrogateopt.html, 2021. Online, accessed May 12th 2021 .
[21] Invernizzi CM. Prospects of mixtures as working fluids in real-gas brayton cycles. Energies 2017;10:1649.
[22] Crespi F, Sánchez D, Sánchez T, Martínez GS. Capital cost assessment of concentrated solar power plants based on supercritical carbon dioxide power cycles. J Eng Gas Turbines Power 2019;141.
[23] Di Marcoberardino G, Invernizzi C, Iora P, Ayub A, Di Bona D, Chiesa P, Binotti M, Manzolini G. Experimental and analytical procedure for the characterization of innovative working fluids for power plants applications. Appl Therm Eng 2020;178:115513.
[24] NFPA 704: Standard system for the identification of the hazards of materials for emergency response, https://www.nfpa.org/codes-and-standards/all-codes-and-standards/list-of-codes-and-standards/detail?code=704, 2021. Online, accessed May 12th 2021 .
[25] Aspen Plus - leading process simulator software, https://www.aspentech.com/en/products/engineering/aspen-properties, 2011. Online, accessed May 12th 2021 .
[26] Dias AM, Carrier H, Daridon JL, Pamies JC, Vega LF, Coutinho JA, Marrucho IM. Vapor- liquid equilibrium of carbon dioxide- perfluoroalkane mixtures: experimental data and saft modeling. Ind Eng Chem Res 2006;45:2341–50.
[27] Tolley W, Izatt R, Oscarson J. Titanium tetrachloride-supercritical carbon dioxide interaction: a solvent extraction and thermodynamic study. Metallurgical Transactions B 1992;23:65–72.
[28] A. Perdichizzi, G. Lozza, Design criteria and efficiency prediction for radial inflow turbines, in: ASME 1987 international gas turbine conference and exhibition, American Society of Mechanical Engineers Digital Collection.
[29] Aqel O, White M, Khader M, Sayma A. Sensitivity of transcritical cycle and turbine design to dopant fraction in co2-based working fluids. Appl Therm Eng 2021;190:116796.